Alterations in T_1 of Normal and Reperfused Infarcted Myocardium after Gd-BOPTA versus GD-DTPA on Inversion Recovery EPI

Michael F. Wendland, Maythem Saeed, Kirsi Lauerma, Nikita Derugin, Jan Mintorovitch, Friedrich M. Cavagna, Charles B. Higgins

This study tested whether Gd-BOPTA/Dimeg or Gd-DTPA exerts greater relaxation enhancement for blood and reperfused infarcted myocardium. Relaxivity of Gd-BOPTA is increased by weak binding to serum albumin. Thirty-six rats were subjected to reperfused infarction before contrast (doses = 0.05, 0.1, and 0.2 mmol/kg). ΔR1 was repeatedly measured over 30 min. Gd-BOPTA caused greater ΔR1 for blood and myocardium than did Gd-DTPA; clearance of both agents from normal and infarcted myocardium was similar to blood clearance; plots of ΔR1myocardium/ΔR1blood showed equilibrium phase contrast distribution. Fractional contrast agent distribution volumes were approximately 0.24 for both agents in normal myocardium, 0.98 and 1.6 for Gd-DTPA and Gd-BOPTA, respectively, in reperfused infarction. The high value for Gd-BOPTPA was ascribed to greater relaxivity in infarction versus blood. It was concluded that Gd-BOPTA/Dimeg causes a greater ΔR1 than Gd-DTPA in regions which contain serum albumin.

Key words: reperfused myocardial infarction; echo planar MR imaging; MR contrast media; T_1 measurement.

INTRODUCTION

Compartmentalization of contrast media and the equilibration over time between intravascular and extracellular spaces determine the efficacy of MR contrast media. The kinetics of redistribution of these compounds play a major role in predicting the degree of enhancement of a particular tissue region (1, 2).

It has been reported that the longitudinal relaxivity (r1) of Gd-BOPTA/Dimeg in blood plasma is increased over that in aqueous solution from 4.4 to 9.7 s^{-1} mM^{-1} (3). This increased relaxivity is much greater than observed for Gd-DTPA such that in plasma the r1 for Gd-BOPTA/Dimeg is approximately twice that for Gd-DTPA. A weak binding between serum albumin and Gd-BOPTA/Dimeg has been identified (4) as the cause of the elevated relaxivity and the binding affinity has been estimated to be 15 mM in aqueous solutions of serum albumin based on the change in r1 (3). This increase in relaxivity may be used to advantage in imaging tissue with a high blood content or pathologic lesions (i.e., tumors or infarcted tissue) which contain large quantities of interstitial albumin since these zones may exhibit increased enhancement after Gd-BOPTA/Dimeg administration versus that from other available contrast media. Some of the main characteristics of reperfused infarcted myocardium are an expanded extracellular volume compared with normal myocardium, increased interstitial serum albumin content, increased interstitial fluid pressure, and the presence of cells with damaged membranes. The major pathophysiological mechanisms responsible for the increase in interstitial fluid pressure are the accumulation of plasma proteins and impaired function of the lymphatic system.

Accordingly, the following study was conducted to quantify changes in R1 of blood, normal myocardium and reperfused infarcted myocardium after administration Gd-BOPTA/Dimeg and to compare with results obtained after administering the same doses of Gd-DTPA. In reperfused myocardial infarction, it is known that cardiac vasculature becomes very leaky to plasma proteins (5) and serum albumin accumulates in the myocardial interstitium of the injury zone.

MATERIALS AND METHODS

Contrast Media

Gd-DTPA (gadopentetate dimeglumine, Magnevist; Schering AG, Berlin, Germany) was obtained as the clinical formulation containing 0.5 M Gd-DTPA. The preparation, properties, and pharmacokinetics (6) of this agent have been previously described. Briefly, the compound has a low molecular weight (938 daltons, including dimeglumine) and extracellular distribution in most tissues, including myocardium. This agent exhibits no known interactions with proteins, it distributes rapidly throughout the body with generally simple pharmacokinetics (i.e., no remote tissue compartments with slow distribution). It is cleared rapidly from the blood with a plasma half life of approximately 20 min in rodents (6). Gd-DTPA does not bind either to cellular membranes or to any macromolecular plasma components (7).

Gd-BOPTA/Dimeg (gadobenate dimeglumine; Bracco SpA, Milan, Italy) was obtained from Bracco SpA, Milan, Italy, in septum-sealed vials containing the compound at a 0.5 M concentration. The synthesis (8), physicochemi-

MRM 37:448–456 (1997)

From the Department of Radiology, University of California, San Francisco, CA, (M.F.W., M.S., K.L., N.D., J.M., C.B.H.) and Bracco SpA, Milan, Italy (F.M.C.).

Address correspondence to: Michael F. Wendland, Ph.D., Department of Radiology, University of California, 505 Parnassus Ave, San Francisco, CA 94143-0628.

Received November 20, 1995; revised September 5, 1996; accepted September 6, 1996.

This study was supported by a research grant from Bracco SpA, Milan, Italy.

Presented in part at the 12th Annual Meeting of the Society of Magnetic Resonance in Medicine, New York, NY (1993).

Current address (K.L.): Department of Radiology, Helsinki University Central Hospital, Helsinki, Finland.

Current address (J.M.): VA Medical Center, Cardiovascular MRI Unit, 11301 Wilshire Blvd, Los Angeles, CA 90073

0740-3194/97 $3.00

cal (3), and pharmacokinetic (9) properties of this agent have been described previously. Gd-BOPTA/Dimeg has a similar molecular weight to Gd-DTPA (1060 daltons including dimeglumine) and distributes rapidly to extracellular compartments in most tissues. Its plasma clearance in rats has been characterized as biexponential with characteristic α and β coefficients of 5 and 22 min. Approximately 52% of an intravenously injected dose is cleared via the biliary system in rats (3).

The reported relaxivities for Gd-BOPTA/Dimeg at 20 MHz in 0.15 *M* NaCl solution are 4.4 $mM^{-1}\ s^{-1}$ for r1 and 5.6 $mM^{-1}\ s^{-1}$ for r2, similar to values for Gd-DTPA (3.7 and 5.6 $mM^{-1}\ s^{-1}$, respectively for r1 and r2). However, in heparinized human plasma r1 and r2 for Gd-BOPTA/Dimeg are greatly increased, to 9.7 and 12.5 $mM^{-1}\ s^{-1}$ (3); while r1 Gd-DTPA is only moderately increased, to 4.9 $mM^{-1}\ s^{-1}$. The higher relaxivity of Gd-BOPTA/Dimeg over Gd-DTPA is due to weak binding between the Gd-BOPTA/Dimeg and plasma proteins (3, 4).

Animal Preparation

Sprague-Dawley rats (n = 36) were anesthetized (50 mg/kg sodium pentobarbital), and mechanically ventilated after tracheotomy. A femoral vein was catheterized for delivery of contrast media. The chest was opened at the 4th intercostal space and a snare ligature was placed around the anterior branch of the left main coronary artery. The ligature was tightened to effect occlusion of the artery. In this preparation, the coronary artery is embedded within the myocardium and is not visible (10). The ligature encloses a small portion of myocardium which surrounds the vessel; therefore, successful occlusion is inferred by observing a zone of cyanosis along the anterior wall of the left ventricle distal to the occlusion site. Occlusion was maintained for 60 min before the ligature was loosened and removed to effect reperfusion. Successful reperfusion was verified by observing return of blood flow to the cyanotic zone. Reperfusion was maintained for 1 to 2 h before administration of contrast agent. This duration of occlusion and reperfusion was designed to produce a severe myocardial infarction (11, 12) with sufficient reperfusion duration to allow accumulation of serum proteins in the interstitium of the reperfused infarcted territory.

Magnetic Resonance Imaging

Copper leads were inserted into a forelimb and the lower abdomen and connected to an ECG monitor to provide cardiac gating. Each rat was placed supine in a birdcage resonator (5.6 cm diameter) and the heart was centered in the magnet (Bruker Omega 2.0 T system equipped with Accustar shielded gradients; Bruker Instruments, Inc., Fremont, CA). Magnetic field was optimized by shimming on the image section.

ECG-gated axial inversion recovery echo planar imaging was employed to measure T_1 values of LV chamber blood, normal myocardium and reperfused infarcted myocardium. A blipped EPI sequence was used with the following acquisition parameters: $TR \geq 7.0$ s, TE = 10 ms, matrix = 64 × 64 data points acquired in 32.7 ms, slice thickness = 2 mm, and FOV = 50 × 50 mm. Preparatory nonselective spin inversion was accomplished by a composite (90*x*-180*y*-90*x*) radiofrequency pulse followed by gradient spoiling of residual transverse magnetization. Before EPI, the inversion pulse was carefully calibrated for the slice location by maximizing the spin echo amplitude after a slice-selective pulse in a conventional hard inversion spin echo sequence. T_1 values were derived from measurement of the inversion recovery null point (TI_{null}) by using the equation $T_1 = TI_{null}/\ln 2$. The null point was determined from a set of fully relaxed images in which the TI setting was incremented through a range of values such that at least three negative and three positive image intensities (SI $\leq$ 35% of fully relaxed intensity) were recorded for each region of interest. A delay following the ECG-derived R-wave trigger pulse was used to compensate changes in the TI setting such that all images were obtained at the same phase of the cardiac cycle. This set of images was typically acquired within a time interval of less than 3 min.

Experimental Protocol

Rats were divided into six groups (n = 6 per group). Each group was administered either Gd-DTPA or Gd-BOPTA/Dimeg at doses of 0.05, 0.1, or 0.2 mmol/kg. In each case the injected volume was 1.0 ml/kg. T_1 values were measured before administering the contrast agent and at 4, 9, 14, 19, 24 and 29 min afterward. These values refer to the time elapsed at the middle of each set of inversion recovery images. After imaging was complete, the rats were sacrificed by lethal injection of saturated potassium chloride solution, the hearts removed, sectioned (short axis sections) and stained in triphenyltetrazolium chloride (TTC) to define the infarcted region. TTC staining was used only to confirm the presence and approximate location of myocardial infarction.

Data Analysis

Reconstructed images were identically scaled and converted from a 32-bit float to an 8-bit integer format and transferred to a Macintosh II computer. Images were interpolated to 128 × 128 and region-of-interest (ROI) analysis was performed by using an image analysis program (Image, Wayne Rasband, NIH). Intensity measurements were obtained from myocardium (infarcted and uninfarcted regions) and LV chamber blood. The background noise level was typically between 5 and 10 units with maximal image intensities of 220–250 intensity units.

Statistics

All values are expressed as mean ± SEM The significance of differences between group mean values was determined by analysis of variance (ANOVA) and deemed to be significant with $P < 0.05$. Evaluation of the significance of changes over time of any measured quantity was evaluated by a one-way repeated measures ANOVA model, with subsequent multiple comparisons by using either Sheffe's F or Tukey's T test. In evaluating the effect of dose of a particular agent on measured values, a multi-way repeated measures model was used

initially and further tests were performed only if differences between groups were found to be significant.

RESULTS

Before administration of contrast media, apparent basal T_1 values for regions of interest (LV chamber blood, infarcted and uninfarcted myocardium) were not different ($P > 0.3$) among the six groups of animals (Tables 1 and 2) and were similar to published values (13, 14). Administration of all doses of each contrast media caused significant ($P < 0.05$) reduction in T_1 values of all three regions (Tables 1 and 2). In each case the relative magnitude of ΔR1 ($1/T_1$post - $1/T_1$pre) for these regions followed the order: reperfused infarcted myocardium > LV blood > uninfarcted myocardium (Figs. 1–3). These differences were significant on individual 2-way repeated measures ANOVA tests for each dose of both agents and allowed easy identification of the reperfused infarcted zone in each animal (Fig. 1), which was similar in location and extent to the infarction zone observed on TTC stained sections. Increasing the dose of both agents caused significant increases in ΔR1 for all three regions (Figs. 2 and 3).

In general, the ΔR1 value for each region was maximal at 4 min and thereafter decreased with time after administration of contrast agent (Figs. 2 and 3). Consequently an apparent clearance half-time (i.e., half-time for ΔR1 decrease) for each region could be estimated. For this estimation ΔR1 values in the time course were normalized to the initial value at 4 min postinjection and the resultant curves were fit to a double exponential function. The fit curves (not shown) were used only to estimate the time at which the initial ΔR1 had declined by half. The apparent clearance of Gd-BOPTA/Dimeg from the blood was significantly faster than that of Gd-DTPA (Table 3). Clearance of neither agent was altered significantly by increasing the dose. The apparent clearance half-times for normal myocardium were similar to values for blood with the respective agent and was not altered by increasing the dose (Table 3). The apparent clearance of Gd-DTPA from reperfused infarcted myocardium was also similar to that from blood, indicating that contrast agent is not sequestered in the injury zone in this preparation. However, the clearance of Gd-BOPTA/Dimeg from reperfused infarction was slower than from either blood or myocardium (Table 3).

The similarities in clearance are depicted in plots of ΔR1myocardium/ΔR1blood (Fig. 4), which were constant over time for normal myocardium. Increasing the dose of Gd-DTPA had no effect on the value of this ratio; however, with Gd-BOPTA/Dimeg the largest dose produced significantly smaller values for ΔR1myocardium/ΔR1blood (0.32 ± 0.02) than did the lower doses (0.44 ± 0.02, and 0.43 ± 0.03, respective time averaged values for doses of 0.1 and 0.05 mmol/kg, $P < 0.05$). Analogous plots for reperfused infarction were also constant over time for animals that received Gd-DTPA and the value of ΔR1myocardium/ΔR1blood did not change with dose (Fig. 4, bottom); however, the value for this ratio was much larger than that observed for normal myocardium. In animals that received Gd-BOPTA/Dimeg, the ΔR1 ratio

Table 1
T_1 Values (s) Measured after Administration of Gd-DTPA (n = 6)

Time (min)	Dose (mmol/kg)	LV blood	Region	
			Normal myo	Infarcted myo
	0.05			
pre		1.36 ± 0.03	0.95 ± 0.02	1.14 ± 0.02
4		0.70 ± 0.04	0.74 ± 0.02	0.54 ± 0.04
9		0.80 ± 0.04	0.80 ± 0.02	0.60 ± 0.04
14		0.86 ± 0.05	0.83 ± 0.02	0.65 ± 0.03
19		0.91 ± 0.05	0.84 ± 0.02	0.68 ± 0.02
24		0.95 ± 0.05	0.85 ± 0.02	0.72 ± 0.02
29		0.98 ± 0.05	0.86 ± 0.02	0.73 ± 0.02
	0.1			
pre		1.35 ± 0.03	0.97 ± 0.01	1.18 ± 0.03
4		0.40 ± 0.04	0.58 ± 0.03	0.28 ± 0.03
9		0.46 ± 0.05	0.62 ± 0.03	0.32 ± 0.03
14		0.52 ± 0.06	0.64 ± 0.04	0.36 ± 0.04
19		0.58 ± 0.07	0.67 ± 0.04	0.40 ± 0.05
24		0.61 ± 0.09	0.70 ± 0.04	0.43 ± 0.07
29		0.63 ± 0.09	0.71 ± 0.05	0.45 ± 0.07
	0.2			
pre		1.32 ± 0.03	0.94 ± 0.01	1.16 ± 0.02
4		0.24 ± 0.02	0.44 ± 0.02	0.15 ± 0.01
9		0.31 ± 0.02	0.50 ± 0.02	0.19 ± 0.01
14		0.33 ± 0.02	0.53 ± 0.01	0.21 ± 0.01
19		0.36 ± 0.02	0.56 ± 0.01	0.24 ± 0.02
24		0.38 ± 0.02	0.58 ± 0.02	0.26 ± 0.02
29		0.40 ± 0.03	0.59 ± 0.02	0.27 ± 0.02

Table 2
T_1 Values (s) Measured after Administration of Gd-BOPTA/Dimeg (n = 6)

Time (min)	Dose (mmol/kg)	LV blood	Region	
			Normal myo	Infarcted myo
	0.05			
pre		1.29 ± 0.04	0.96 ± 0.02	1.11 ± 0.02
4		0.50 ± 0.04	0.65 ± 0.03	0.32 ± 0.03
9		0.66 ± 0.07	0.73 ± 0.03	0.40 ± 0.04
14		0.76 ± 0.07	0.77 ± 0.03	0.43 ± 0.05
19		0.81 ± 0.08	0.78 ± 0.03	0.48 ± 0.05
24		0.91 ± 0.08	0.83 ± 0.03	0.56 ± 0.06
29		0.94 ± 0.10	0.85 ± 0.03	0.60 ± 0.07
	0.1			
pre		1.35 ± 0.04	0.98 ± 0.03	1.20 ± 0.03
4		0.34 ± 0.04	0.53 ± 0.05	0.20 ± 0.04
9		0.48 ± 0.06	0.61 ± 0.05	0.26 ± 0.04
14		0.57 ± 0.07	0.66 ± 0.05	0.31 ± 0.04
19		0.63 ± 0.07	0.69 ± 0.04	0.37 ± 0.04
24		0.69 ± 0.08	0.72 ± 0.04	0.40 ± 0.04
29		0.73 ± 0.08	0.74 ± 0.04	0.44 ± 0.04
	0.2			
pre		1.29 ± 0.03	0.92 ± 0.02	1.14 ± 0.03
4		0.19 ± 0.02	0.42 ± 0.03	0.12 ± 0.01
9		0.29 ± 0.06	0.51 ± 0.05	0.13 ± 0.02
14		0.37 ± 0.07	0.56 ± 0.05	0.16 ± 0.03
19		0.42 ± 0.08	0.61 ± 0.05	0.19 ± 0.03
24		0.47 ± 0.09	0.62 ± 0.05	0.22 ± 0.04
29		0.51 ± 0.09	0.65 ± 0.06	0.25 ± 0.04

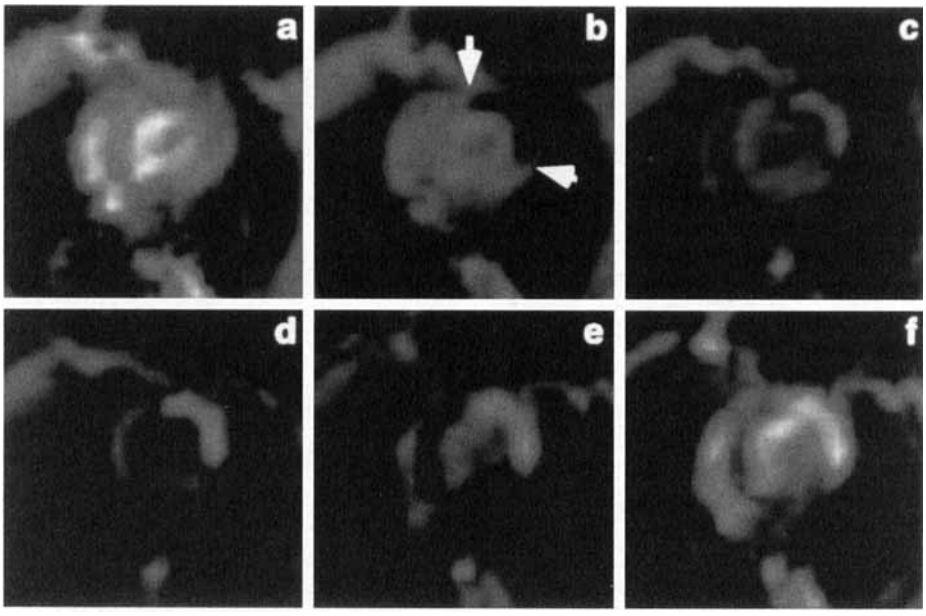

FIG. 1. R1 measurement in one animal. Images were obtained 24 min after administration of 0.1 mmol/kg Gd-BOPTA/Dimeg. TI settings for these images were: (a) 0.05, (b) 0.15, (c) 0.25, (d) 0.3, (e) 0.4, and (f) 0.6 s. All images are displayed in magnitude intensity form, with all regions exhibiting negative intensity at TI = 0.05 s and positive intensity at TI = 0.6 s. Regions with larger R1 values demonstrate null intensity at smaller TI settings, thus R1 of reperfused infarction (arrows) > R1 of chamber blood > R1 of normal myocardium. These images were all zoomed once to the region of the heart and then interpolated. Images thus depict raw data matrices of 32 × 32 points. Note that the reperfused infarction in (c) is surrounded by a null boundary (one pixel wide on uninterpolated images), which aids assignment of regional signal polarity when signal approaches the null point.

for reperfused infarction exhibited an initial increase in value during the first 10 min after administration and thereafter did not change during the remaining observation period (Fig. 4, top). This profile was the same for all doses of Gd-BOPTA/Dimeg. The value of the ΔR1 ratio in the constant region of the curve was significantly greater than that for normal myocardium in animals that received Gd-BOPTA/Dimeg and was also significantly greater than values observed for reperfused infarction in animals that received Gd-DTPA (Fig. 4). Finally, ΔR1 of reperfused infarction relative to that of normal myocardium was significantly greater in animals that received Gd-BOPTA/Dimeg versus animals that received Gd-DTPA (Fig. 5), indicating that contrast between normal and reperfused infarcted myocardium would be greater by using Gd-BOPTA/Dimeg.

DISCUSSION

The major limitation associated with this study is related to the method of T_1 measurement during the clearance phase of contrast media. In selecting a method for T_1 estimation it was considered important to determine T_1 from as few measurements as possible since the contrast agent concentration, and hence the T_1 values, were changing with time during clearance. It was also important to avoid error from T_2 decreases that accompany contrast media and confound T_1 calculation from signal intensity change in individual images. Consequently, the compromise solution used in the current study was to estimate the inversion recovery null point, which is insensitive to T_2 error and greatly reduces the temporal error caused by the effects of clearance on the inversion recovery profile. Temporal misregistration for zones with different T_1 values is still present because null intensity was not observed at the same time for each region. This error was not large because observation of null intensity for the region with smallest T_1 (reperfused infarction) was always within 60 s of that for the region with greatest T_1 (usually normal myocardium). This temporal offset is small compared with the clearance time for agents used in this study, and error that propagates into ΔR1 ratio values is considered negligable.

Reperfusion of infarcted myocardium initiates a progression of changes in the myocardium both at the cellular and tissue levels that have a pronounced impact on the influence of exogenous MR contrast media on R1 of the damaged zone, and consequently on signal intensity of T_1-weighted MR images. Early after reflow is established, irreversibly injured myocardium undergoes explosive cellular swelling caused by re-establishment of normosmotic extracellular conditions while the intracellular fluid is hyperosmotic from ion imbalance during ischemia (15). Membrane damage from cellular swelling as well as potential enzymic activation of phospholipases during intracellular calcium overload and free radical damage during initial reperfusion causes a failure of membrane integrity. With the failure of membrane integrity, low molecular weight exogenous contrast media are no longer excluded from the cellular spaces (16, 17). The available distribution volume and hence the quantity of MR contrast medium per pixel are increased. Secondly, damage to the microvascular endothelium occurs leading initially to increased leakage of macromol-

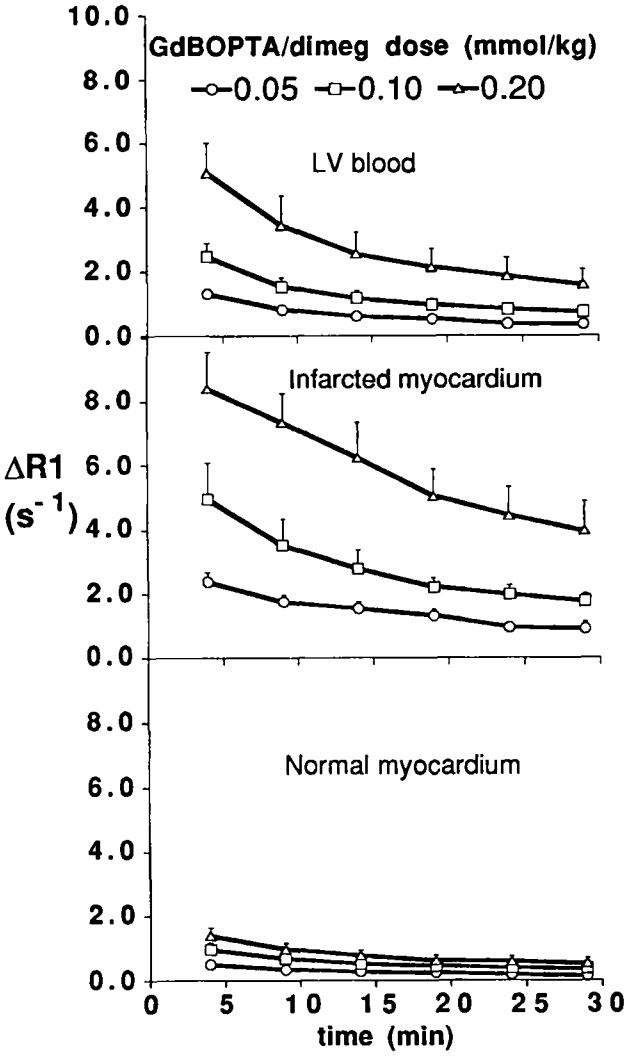

FIG. 2. Change in ΔR1 of left ventricle chamber blood, infarcted myocardium and normal myocardium after administration of Gd-BOPTA/Dimeg to six rats subjected to 60 min left coronary occlusion and reflow. Note that ΔR1 of reperfused infarcted myocardium is greater than that in blood and normal myocardium, and decreases with time for all three regions.

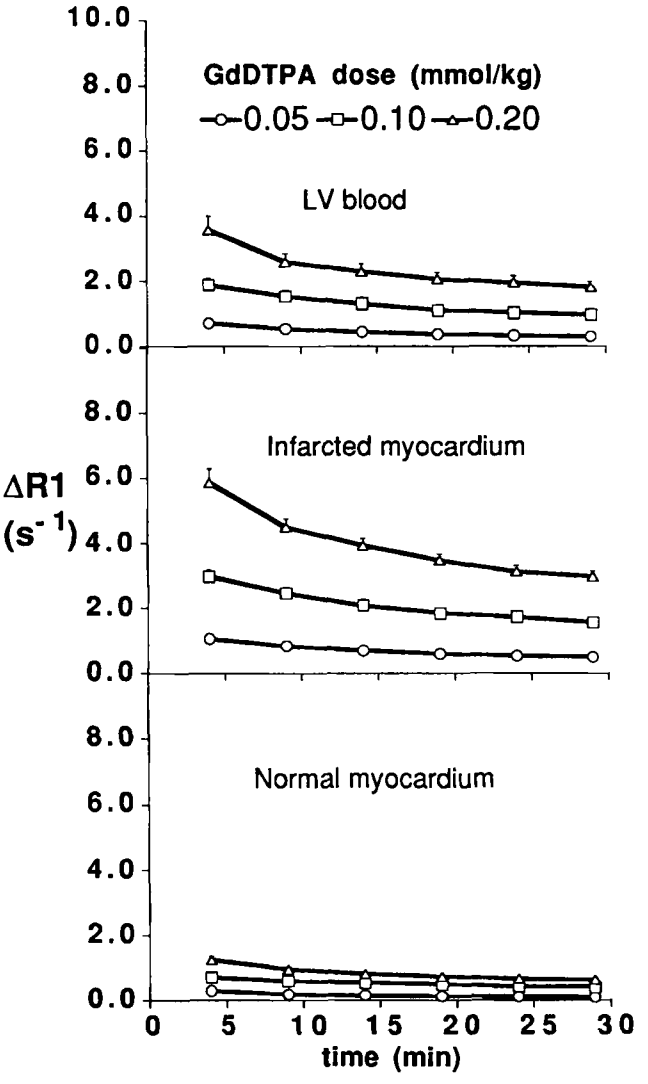

FIG. 3. Change in ΔR1 of left ventricle chamber blood, infarcted myocardium and normal myocardium after administration of Gd-DTPA to six rats subjected to 60 min left coronary occlusion and reflow. Note that (a) similar to animals that received Gd-BOPTA/Dimeg, reperfused infarcted myocardium demonstrated greatest change in R1 while smaller changes were evident for chamber blood and normal myocardium; (b) all regions demonstrated similar declines in ΔR1 over time; and (c) ΔR1 values were generally less than in animals that were given Gd-BOPTA/Dimeg.

ecules into the interstitium of the injured territory (18). This combined with the liberation of intracellular proteins increases the osmolarity in the interstitium and consequently interstitial edema evolves. Interstitial edema also enlarges the distribution volume of contrast media. It is thought that progressive swelling of the tissue ultimately compresses the microvasculature to the extent that perfusion is eventually blocked at the microvascular level producing the "no-reflow" phenomenon (19, 20).

On MR imaging reperfused myocardial infarction is typically characterized by intense postcontrast signal enhancement on T_1-weighted sequences (21–25). The enhancement is usually very homogeneous and persists for more than 1 h after administering contrast media, and little notable decrease in signal enhancement is observed during this 1st h (22–25). To the contrary, normal myocardium exhibits a maximal enhancement early after administration followed by decreasing enhancement with time after injection reflecting clearance of the agent from the circulation (22–25). These temporal features have led to the hypothesis that the contrast agent is sequestered in the reperfused infarcted zone by a combination of enlarged distribution volume and poor perfusion in the damaged territory (21, 22, 24, 25). Indeed, in this model it has been shown that the first pass profile for T_1-enhancing MRI media is reduced compared with that of normal myocardium followed by continued slow increase in signal (26), supporting the hypothesis of diminished flow and slow accumulation of agent in the injury zone.

The results from the current study suggest that the former view is not entirely correct. While perfusion may be reduced in the reperfused infarcted territory, it is not

Table 3
Clearance Half-Time Values (min) for Gd-DTPA and Gd-BOPTA/Dimeg

	n[a]	LV blood	Normal myocardium	Reperfused infarcted myocardium
Gd-DTPA 0.05 mmol/kg	5	18 ± 3	16 ± 3	21 ± 4
Gd-BOPTA 0.05 mmol/kg	5	10 ± 2[b]	13 ± 3	18 ± 3[c]
Gd-DTPA 0.1 mmol/kg	6	23 ± 4	24 ± 4	22 ± 4
Gd-BOPTA 0.1 mmol/kg	5	10 ± 2[b]	13 ± 2[b]	19 ± 5[c]
Gd-DTPA 0.2 mmol/kg	5	21 ± 3	23 ± 2	18 ± 2
Gd-BOPTA 0.2 mmol/kg	4	10 ± 2[b]	11 ± 2[b]	19 ± 4[c]

[a] n was reduced from 6 as shown because in each group there was usually at least one case in which clearance from the blood was exceedingly slow (i.e., >35 min) and a clearance half-time could not be accurately measured. These cases were excluded from consideration of clearance but were included in all other evaluations; the apparent linearity of temporal values of ΔR1ratio was not affected by the slow blood clearance (i.e., clearance from myocardium was equally slow as that from blood).
[b] $P < 0.05$ in comparison with values obtained with Gd-DTPA on unpaired two-tailed Students t test.
[c] $P < 0.05$ in comparison with value obtained for blood on paired two-tailed Student's t test.

sufficiently slow to kinetically sequester contrast agent in the reperfused infarcted territory from that in the central blood pool in this model. Apparent clearance from reperfused infarcted myocardium was largely unimpeded compared with clearance from central blood. This finding was unanticipated but is consistent if one considers that the only requirement for apparent unimpeded clearance is that contrast media in the reperfused infarction must mix with that in the central blood plasma more quickly than the agent is cleared from the plasma, and plasma clearance is a rather slow process. The previous findings that signal enhancement of reperfused myocardium is nearly constant over 60 min after contrast administration can be explained if T_1 of the reperfused infarcted zone is sufficiently short that the region is nearly fully relaxed (i.e., $TR \geq 3 * T_1$) for all postcontrast images, such that real reduction of contrast agent over time is simply not observed.

Evaluation of ΔR1Myocardium/ΔR1blood Values

The expression of the measured data as ΔR1myocardium/ΔR1blood and its temporal changes provides a highly informative perspective of contrast distribution in the myocardium and of the physiologic status of the tissue, particularly in regions of myocardial damage. In the absence of accurate blood data, such as in a spin-echo

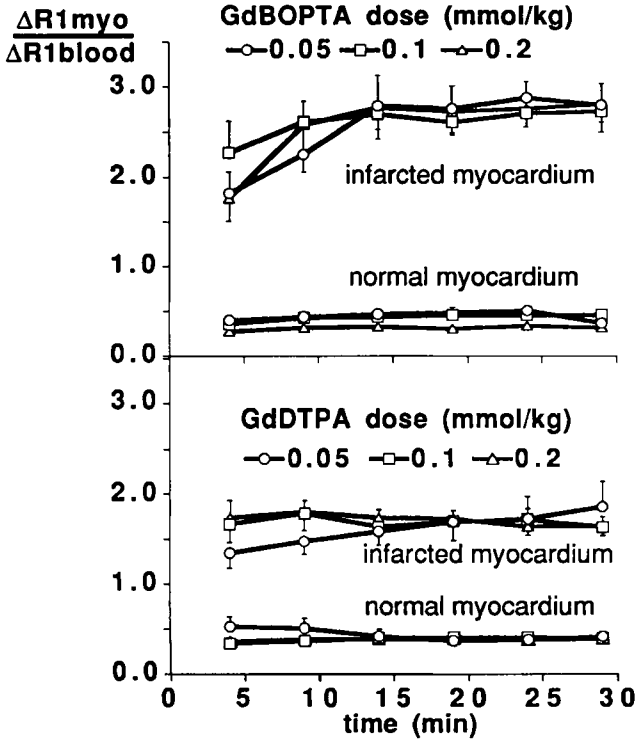

FIG. 4. Change in ΔR1myocardium/ΔR1blood after administration of Gd-BOPTA/Dimeg and Gd-DTPA. Notice that all regions demonstrate no dose dependence and either constant values for the ΔR1 ratio or initial rise to a constant value (reperfused infarction in animals given Gd-BOPTA/Dimeg) suggesting equilibrium phase contrast distribution between myocardium and blood.

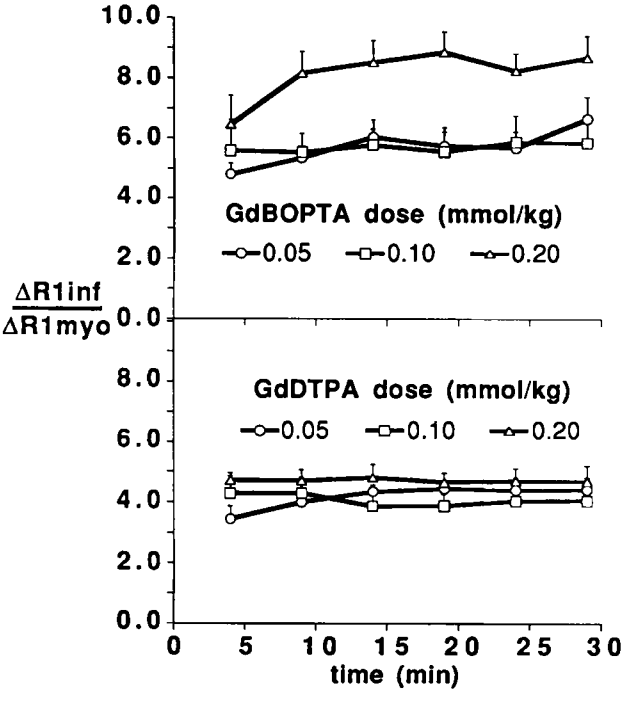

FIG. 5. Change in ΔR1infarct/ΔR1normal myocardium after administration of Gd-BOPTA/Dimeg and Gd-DTPA. Notice that animals that received Gd-BOPTA/Dimeg exhibit significantly larger values for this ratio than animals that received Gd-DTPA, indicating that Gd-BOPTA/Dimeg would provide greater contrast between normal and reperfused infarcted regions on T_1-weighted MRI.

acquisition, comparison of ΔR1 ratios at different myocardial regions also provides a useful index.

To evaluate the ΔR1 ratio plots, we use an approximate pharmacokinetic description of contrast agent distribution in perfused myocardium that is appropriate to the experimentally measured quantities:

$$[CM]_{myo} \underset{k_{efflux}}{\overset{k_{influx}}{\leftrightarrows}} [CM]_{pl} \overset{k_c}{\rightarrow\rightarrow} \quad [1]$$

where CM is contrast media, "myo" and "pl" refer to myocardium and blood plasma, respectively, k_{influx} and k_{efflux} refer to rate constants for influx of contrast media from blood to myocardium and efflux from myocardium to blood, and k_c refers to the plasma clearance rate constant. In this model, all of the rate constants "k" are summary constants in that none represents a single process. k_{influx} and k_{efflux} contain contributions from (a) the exchange of blood between the local tissue blood compartment and the central circulation (perfusion); (b) the traversal of CM across the capillary wall (i.e., permeability surface area product); and (c) the mixing of CM within the interstitium (diffusion). In normal myocardium it is assumed that blood flow and intracompartment mixing do not appreciably limit influx and efflux of extravascular contrast media but in injured myocardium the validity of these assumptions is doubtful and supportive experimental evidence is required. k_c characterizes the combined processes of endpoint clearance via biliary and renal systems and exchange into remote tissue (muscle, gut, and other organs) compartments which buffers the central plasma concentration during clearance. It is assumed that myocardial interstitium is very small compared with the remaining whole body distribution volume for contrast agent and therefore back diffusion of CM from myocardium to blood contributes negligibly to the central plasma concentration.

The change in R1 of myocardium and blood can be approximately related to change in contrast media concentration as:

$$\Delta R1_{myo} = [CM]myo \times r1_{myo} \quad [2]$$

$$= [CM]_{ECV} \times fECV \times r1myo$$

$$\Delta R1_{blood} = [CM]blood \times r1_{blood} \quad [3]$$

$$= [CM]pl \times (1.0 - Hct) \times r1_{blood}$$

where fECV refers to the fractional extracellular volume, Hct is the blood hematocrit, and $r1_{myo}$ and $r1_{blood}$ refer respectively to local longitudinal relaxivities for contrast medium in myocardium and blood. These expressions assume that intercompartment mixing of tissue water is very rapid, and current evidence indicates this is not true for mixing between intravascular and extravascular water compartments within myocardium (14, 27–29). However, with contrast media present in both vascular and extravascular compartments, relaxation rates would be similar and slow water exchange would not appreciably limit the overall rate (30). Then, dividing Eq. [2] by Eq. [3] (31):

$$\Delta R1myo/\Delta R1blood = [CM]_{ECV}/[CM]pl \times fECV/(1 - Hct) \times r1_{myo}/r1_{blood} \quad [4]$$

where the ΔR1 ratio is expressed as the product of the ratios of (a) concentration of agent in the myocardium to that in blood distribution volumes, (b) the fractional distribution volumes in myocardium to whole blood, and (c) the respective local longitudinal relaxivities of contrast agent in the two compartments. Any possible limiting effect of water exchange between intracellular and extracellular compartments on relaxation is included in the local relaxivities. This is appropriate because any departure from monoexponential relaxation would not be observable in this measurement since (a) complete relaxation profiles were not obtained, (b) signal-to-noise ratio was sufficient to detect only great departure from monoexponential behavior (32), and (c) R1 was changing with time while measurements were being recorded.

After contrast media is administered, its concentration in the plasma initially exceeds that in the myocardial interstitium. Since [CM]pl × kin > $[CM]_{ECV}$ × kout, there is a net increase of [CM]myo with time until the condition is reached that [CM]pl × kin = [CM]myo × kout. This initial process can be considered the tissue loading phase and in normal myocardium this process is complete within the first minutes after contrast administration. Subsequent clearance of CM from the plasma causes net clearance of CM from the tissue. If kin ≈ kout ≫ kc, then clearance of CM from the myocardium will very nearly keep pace with plasma clearance and $[CM]_{ECV}$/[CM]pl ≈ kin/kout. Alternatively, if kin≈kout≈kc, clearance of CM from tissue will lag that from plasma and $[CM]_{ECV}$/[CM]pl will increase with time until [CM]pl approaches zero (14). The former circumstance is more consistent with the results of the current study. Finally, since movement of CM between blood and tissue compartments is passive rather than facilitated, it is assumed that kin = kout. Eq. [4] can be simplified and rearranged to:

$$\Delta R1myo/\Delta R1blood \times (1.0 - Hct) = fECV \times r1_{myo}/r1_{blood} \quad [5]$$

It is noteworthy that (a) fECV includes the myocardial blood plasma volume within each pixel and that the distribution volume is not a true volume but is taken to be the fraction of total MR observable water within each pixel that is contained in the space available for contrast media distribution; and (b) this expression is applicable only if $[CM]_{ECV}$/[CM]pl is equal to 1, a condition that is supported by ΔR1myo/ΔR1blood being constant over some interval of time and insensitive to administered dose.

In normal (uninfarcted) myocardium, the ΔR1myo/ΔR1blood ratio observed after Gd-DTPA was approximately 0.4, regardless of the injected dose and time after administration. Assuming Hct to be approximately 0.4, the product of ΔR1myo/ΔR1blood and (1 - Hct), is approximately 0.24. This value is less than expected for normal myocardium. The fractional distribution volume

in myocardium of ^{153}Gd-DTPA or tracers with similar molecular weight is typically between 0.3 and 0.4 (33, 34). The expected ΔR1 ratio would be 0.5 to 0.7 rather than 0.4 if the ratio of local relaxivities, r1myo/r1blood, is unity. The true cause of this discrepancy is unknown, but possible explanations might be that (a) values obtained from sacrificed animals, as in radioisotope experiments, may be higher than in living animals since the myocardial blood volume can increase appreciably depending upon the manner of sacrifice; and (b) the ΔR1 method may give an erroneously low value because r1 myo is limited by water exchange between intracellular and extracellular spaces. While it is true that departure from monoexponential relaxation is not usually apparent after quite high doses of Gd-DTPA, the local r1 would be reduced appreciably before compartmentalization is evident as biexponential relaxation.

In reperfused infarction the ΔR1 ratio value was constant with time after administration of Gd-DTPA and was independent of dose, therefore it is likely that kin, kout $\gg$ kc. If the r1 ratio is unity, then the apparent fECV is $0.6 \times 1.63 \approx 0.98$, indicating that virtually all of the myocardial cellular volume in the injury zone is within the distribution volume of the contrast agent, probably indicating lethal cell membrane damage. This finding is important because it suggests a method for quantifying the necrotic cell fraction within the infarcted territory which may be less than 100% (12) in less severe injury.

The results obtained with Gd-BOPTA/Dimeg are more difficult to rationalize. It was true that generally greater ΔR1 values were noted in the blood pool after administering Gd-BOPTA/Dimeg as compared with Gd-DTPA (2.46 ± 0.4 versus 1.88 ± 0.2), in accord with the known effect of serum albumin on r1 in blood, but increases were also noted in ΔR1 values of myocardium (0.96 ± 0.2 versus 0.72 ± 0.1). Thus, a significant difference between ΔR1 ratio values was not obtained. However, one would expect that ΔR1 of myocardium would be dominated by Gd-BOPTA/Dimeg in the interstitium rather than by that in the myocardial blood because (a) the interstitial volume is larger than the blood volume and (b) limited transcapillary exchange of water would reduce the access of most of the tissue water, that in the cellular spaces, to the intravascular compartment. Since there is very little albumin present in interstitium of normal myocardium, $r1_{blood}$ is expected to be greater than r1 myocardium which in turn should cause lower ΔR1myo/ΔR1blood values than obtained with Gd-DTPA. Why was this expected lowering of the ΔR1 ratio only found at a dose of 0.2 mmol/kg and not at the lower doses? We can only speculate that transcapillary exchange of water is sufficiently fast that at the lower doses the higher relaxation rate in the tissue blood penetrates into the extravascular compartment. This is not a very satisfactory explanation because when the agent was cleared from the blood after the higher dose, the ΔR1 ratio did not increase toward the value observed at the lower doses.

In reperfused infarcted myocardium, the ΔR1 ratio exhibited an initial rise to a constant high value suggesting an approach to equilibrium phase distribution. The ΔR1 value in the constant portion was much higher than noted for Gd-DTPA. If we assume that equilibrium distribution exists in this portion of the curve, then the fECV-r1 ratio product (i.e., right hand side of Eq. [5]) is approximately $2.7 \times 0.6 = 1.62$. Obviously, the fECV cannot be greater than 1.0 forcing the r1myo/r1blood ratio to at least a value of 1.6. This value for r1 ratio cannot be explained solely on the basis of serum albumin accumulation in the reperfused infarcted tissue. Albumin concentration in the extravascular compartment cannot be higher than in plasma since plasma is its only source. Thus, the ratio of relaxivities of Gd-BOPTA/Dimeg in tissue to that in blood should not exceed unity unless there is a change in bound-site relaxation rate (meaning relaxation rate of water ligated to gadolinium) or a change in fraction of Gd-BOPTA/Dimeg that is bound to protein. Since myocardial intracellular proteins are available for interaction with Gd-BOPTA in the damaged territory, it seems most sensible to ascribe the apparent elevation of Gd-BOPTA/Dimeg relaxivity in the tissue to an increased fraction of bound Gd-BOPTA/Dimeg in this region.

CONCLUSIONS

The important findings of this study were that (a) when administered at similar dose levels, Gd-BOPTA/Dimeg causes greater increases in R1 than provided by Gd-DTPA consistent with its known larger r1 relaxivity of the former agent in solutions containing serum albumin. This effect is particularly important in reperfused infarcted myocardium where plasma proteins are known to accumulate and greater potential contrast between reperfused infarction and normal myocardium would be available for T_1-weighted imaging; (b) ΔR1 values were greatest in reperfused infarcted myocardium, less in chamber blood, and least in normal myocardium throughout the observation, and the agent was cleared efficiently from all myocardial regions indicating that the contrast agent is not sequestered in reperfused myocardial infarction for this preparation; (c) the ratio of ΔR1 values in tissue to that in blood were consistent with a Gd-DTPA distribution volume containing 24% of myocardial water (including myocardial blood volume) in normal or uninjured myocardium and nearly 100% in hearts subjected to reperfused infarction. This finding suggests that the ΔR1 ratio can be used to quantify the fraction of viable myocardial cells present in reperfused infarcted territories containing a mixture of viable and nonviable cells.

REFERENCES

1. H. J. Weinmann, M. Laniado, W. Mutzel, Pharmacokinetics of Gd-DTPA/dimeglumine after intravenous injection into healthy volunteers. *Physiol. Chem. Phys. Med. NMR* **16**, 167–178 (1988).
2. P. Wedeking, M. F. Tweedle, Comparison of the biodistribution of 153Gd-labeled Gd(DTPA)$^{-2}$ and Gd(DOTA) and Gd(acetate) in mice. *Int. J. Rad. Appl. Inst.* **15**, 395–401 (1988).
3. C. de Haën, L. Gozzini, Soluble-type hepatobiliary contrast agents for MR imaging. *J. Magn. Reson. Imaging* **3**, 179–86 (1993).
4. F. M. Cavagna, P. Marzola, M. Dapra, F. Maggioni, E. Vicinanza, P. M. Castelli, C. de Haën, C. Luchinat, M. F. Wendland, M. Saeed, C. B. Higgins, Binding of gadobenate dimeglumine to proteins extravasated into interstitial space enhances conspicuity of reperfused infarcts. *Invest. Radiol.* **29**(Suppl. 2), S50–S253 (1994).
5. K. P. Sunnergren, M. J. Rovetto, Microvascular permeability charac-

teristics of the isolated perfused ischemic rat heart. *J. Mol. Cell. Cardiol.* **12,** 1011–1031 (1980).
6. H. J. Weinmann, R. C. Brasch, W. R. Press, G. E. Wesbey, Characterization of gadolinium-DTPA complex: A potential NMR contrast agent. *Am. J. Roentgenol.* **142,** 619–624 (1984).
7. S. H. Koenig, Medical magnetic resonance: a primer, *in* "Proc., SMRM, 7th Annual Meeting, 1988," p. 111.
8. A. Davies, C. de Haën, Gadobenic acid dimeglumine salt. *Drugs Future* **16,** 1001–1003 (1991).
9. G. Vittendi, E. Felder, P. Tirone, V. Lorusso, B-19036: a potential new hepatobiliary contrast agent for MR proton imaging. *Invest. Radiol.* **23**(Suppl 1), 246–248 (1988).
10. R. E. Sievers, U. Schmiedl, C. L. Wolfe, M. E. Moseley, W. W. Parmley, R. C. Brasch, M. J. Lipton, A model of acute regional myocardial ischemia and reperfusion in the rat. *Magn. Reson. Med.* **10,** 172–81 (1989).
11. S. Hale, R. A. Kloner, Effect of early coronary artery reperfusion on infarct development in a model of low collateral flow. *Cardiovasc. Res.* **21,** 668–673 (1987).
12. C. E. Ganote, R. Seabra-Gomes, W. G. Nayler, R. B. Jennings, Irreversible myocardial injury in anoxic rat hearts. *Am. J. Pathol.* **80,** 419–450 (1975).
13. M. F. Wendland, M. Saeed, T. Masui, N. Derugin, M. E. Moseley, C. B. Higgins, Echo-Planar MR imaging of normal and ischemic myocardium with gadodiamide injection. *Radiology* **186,** 535–542 (1993).
14. M. F. Wendland, M. Saeed, K. K. Yu, T. P. L. Roberts, K. Lauerma, N. Derugin, J. Varadarajan, A. D. Watson, C. B. Higgins, Inversion recovery EPI of bolus transit in rat myocardium using intravascular and extravascular gadolinium-based MR contrast media: dose effects on peak signal enhancement. *Magn. Reson. Med.* **32,** 319–329 (1994).
15. R. Jennings, K. Reime, Lethal myocardial ischemic injury. *Am. J. Pathol.* **102,** 241–255 (1981).
16. J. F. Geschwind, M. F. Wendland, M. Saeed, K. Lauerma, N. Derugin, C. B. Higgins, Identification of myocardial cell death in reperfused myocardial injury using dual mechanisms of contrast enhanced magnetic resonance imaging. *Acad. Radiol.* **1,** 319–325 (1994).
17. M. Saeed, M. F. Wendland, T. Masui, C. B. Higgins, Reperfused myocardial infarctions on T1- and susceptibility-enhanced MRI: evidence for loss of compartmentalization of contrast media. *Magn. Reson. Med.* **31,** 31–39 (1994).
18. D. Garcia-Dorado, P. Theroux, J. Solares, J. Alonso, F. Fernandez-Aviles, J. Elizaga, J. Soriano, J. Botas, R. Munoz, Determinants of hemorrhagic infarcts. Histologic observations from experiments involving coronary occlusion, coronary reperfusion, and reocclusion. *Am. J. Pathol.* **137,** 301–311 (1990).
19. H. Ito, T. Tomooka, N. Sakai, H. Yu, Y. Higashino, K. Fujii, T. Masuyama, A. Kitabatake, T. Minamino, Lack of myocardial perfusion immediately after successful thrombolysis. A predictor of poor recovery of left ventricular function in anterior myocardial infarction. *Circulation* **85,** 1699–1705 (1992).
20. R. A. Kloner, C. E. Ganote, R. B. Jennings, The "no reflow" phenomenon after temporary coronary occlusion in the dog. *J. Clin. Invest.* **54,** 1496–1508 (1974).
21. A. de Roos, A. C. van Rossum, E. van der Wall, S. Postema, J. Doornbos, N. Matheijssen, P. R. van Dijkman, F. C. Visser, A. E. van Voorthuisen, Reperfused and nonreperfused myocardial infarction: diagnostic potential of Gd-DTPA-enhanced MR imaging. *Radiology* **172,** 717–720 (1989).
22. T. Masui, M. Saeed, M. F. Wendland, C. B. Higgins, Occlusive and reperfused myocardial infarcts: MR imaging differentiation with nonionic Gd-DTPA-BMA. *Radiology* **181,** 77–83 (1991).
23. M. Saeed, M. F. Wendland, Y. Takehara, C. B. Higgins, Reversible and irreversible injury in the reperfused myocardium: differentiation with contrast material-enhanced MR imaging. *Radiology* **175,** 633–637 (1990).
24. M. Saeed, M. F. Wendland, C. B. Higgins, Characterization of reperfused myocardial infarctions with T1-enhancing and magnetic susceptibility-enhancing contrast media. *Invest. Radiol.* **26,** S239-S 241 (1991).
25. M. Saeed, M. F. Wendland, Y. Takehara, T. Masui, C. B. Higgins, Reperfusion and irreversible myocardial injury: identification with a nonionic MR imaging contrast medium. *Radiology* **180,** 675–683 (1992).
26. M. Saeed, M. F. Wendland, K. K. Yu, K. Lauerma, H. T. Li, N. Derugin, F. M. Cavagna, C. B. Higgins, Identification of myocardial reperfusion with echo planar magnetic resonance imaging. Discrimination between occlusive and reperfused infarctions. *Circulation* **90,** 1492–501 (1994).
27. K. M. Donahue, D. Burstein, W. J. Manning, M. L. Gray, Studies of Gd-DTPA relaxivity and proton exchange rates in tissue. *Magn. Reson. Med.* **32,** 66–75 (1994).
28. D. Burstein, E. Taratuta, W. Manning, Factors in myocardial "perfusion" imaging with ultrafast MRI and Gd-DTPA administration. *Magn. Reson. Med.* **20,** 299–305 (1991).
29. R. M. Judd, M. K. Atalay, G. A. Rottman, E. A. Zerhouni, Effects of myocardial water exchange on T1 enhancement during bolus administration of MR contrast agents. *Magn. Reson. Med.* **33,** 215–23 (1995).
30. K. M. Donahue, R. M. P. D. J. Weisskoff, R. J. Callahan, R. A. Wilkinson, J. B. Mandeville, B. R. Rosen, Dynamic Gd-DTPA enhanced MRI measurement of tissue cell volume fraction. *Magn. Reson. Med.* **34,** 423–432 (1995).
31. P. D. Dean, P. Niemi, L. Kivisaari, M. Kormano, Comparative pharmacokinetics of gadolinium DTPA and gadolinium chloride. *Invest. Radiol.* **23**(Suppl 1), S258–S260 (1988).
32. R. J. S. Brown. Information available and unavailable from multiexponential relaxation data. *J. Magn. Reson.* **82,** 539–561 (1989).
33. F. S. Prato, G. Wisenberg, T. P. Marshall, P. Uksik, P. Zabel, Comparison of the biodistribution of gadolinium-153 DTPA and technetium-99 M DTPA in rats. *J. Nucl. Med.* **29,** 1683–1687 (1988).
34. L. D. Diesbourg, F. S. Prato, G. Wisenberg, D. J. Drost, T. P. Marshall, S. E. Carroll, B. O'Neill, Quantification of myocardial blood flow and extracellular volumes using a bolus injection of Gd-DTPA: kinetic modeling in canine ischemic disease. *Magn. Reson. Med.* **23,** 239–253 (1992).